Stress change in $YBa_2Cu_3O_{7-\delta}$ close to the superconducting transition

L. X. Cao,[1,2] R. K. Kremer,[1] Y. L. Qin,[3] J. Brötz,[4] J. S. Liu,[5] and J. Zegenhagen[1,2,*]
[1]*European Synchrotron Radiation Facility, B.P. 220, F-38043 Grenoble Cedex, France*
[2]*Max-Planck-Institut für Festkörperforschung, D-70569 Stuttgart, Germany*
[3]*Institut für Festkörperforschung, Forschungszentrum, Jülich GmbH, D-52425 Jülich, Germany*
[4]*FG Strukturforschung, FB Materialwissenschaft, TU-Darmstadt, D-64287 Darmstadt, Germany*
[5]*Institute of Microelectronics, Tsinghua University, Beijing 100084, People's Republic of China*
(Received 12 December 2001; revised manuscript received 3 June 2002; published 8 August 2002)

Measurements on $Au/Pb(Zr_{1-x}Ti_x)O_3/YBa_2Cu_3O_{7-\delta}$ ($x=0.47,0$) thin film capacitor structures on $SrTiO_3(001)$ reveal a jump up to $\approx 30\%$ in the dielectric constant of the ferroelectric $Pb(Zr_{0.53}Ti_{0.47})O_3$ films, which starts about 10 K above the superconducting transition of the underlying $YBa_2Cu_3O_{7-\delta}$ layer. We show that this can be understood by a stress release in the ferroelectric film which must be caused by a stress change in the high-temperature superconductor starting already significantly above T_c.

DOI: 10.1103/PhysRevB.66.054511 PACS number(s): 68.35.−p, 74.76.Bz, 77.55.+f, 77.65.−j

The coupling term between an external field and the order parameter effects the free energy of a superconductor.[1] Compared to the change of the electric and magnetic properties associated with the superconducting transition, the effect on an existing stress field is less well studied. However, for both, conventional superconductors[2,3] and high-temperature superconductors (HTS),[4] it was found experimentally that the superconducting transition is accompanied by an anomaly of the elasticity/plasticity. Although there is no conclusive evidence,[5,6] the changed interaction between moving dislocations and the conduction electrons was suggested to be responsible.[2,3] In this paper, we provide convincing evidence for a stress change in HTS thin film at around the superconducting transition temperature. Intriguingly, the effect is observed to start already at about 10 K above T_c.

It had been found earlier that the superconducting transition in electrode layers of $YBa_2Cu_3O_{7-\delta}$ (YBCO) can effect the dielectric properties of a thin film capacitor with $Ba_{0.5}Sr_{0.5}TiO_3$ or $Pb(Zr_{0.53}Ti_{0.47})O_3$ (PZT) dielectric layers.[7,8] For this observation, e.g., the proximity effect was suggested as an explanation.[7] In the present study, we elucidate the underlying reason by comparing the temperature dependence of the capacitances of ferroelectric (FE) thin film capacitors with those of antiferroelectric (AFE) $PbZrO_3$ (PZ) thin film capacitors. In this way, we can rule out that the observed effect arises simply from the proximity effect, i.e., that the *effective* thickness of the dielectric layer is decreased and therefore the capacitance of the heterostructure is increased in the superconducting state. In order to assure that the observed dielectric anomaly is associated with the superconducting transition and not with the normal state anomalies at temperatures T^* above T_c, notably the pseudogap,[9–11] we prepared PZT/YBCO and PZ/YBCO heterostructures with *underdoped* YBCO films. In this way, we are varying T_c and can see clearly, whether the detected anomaly in the capacitance scales with T_c or not. This is also important in view of the fact that the separation of T_c and T^* on the temperature scale is also a function of the doping level. Thus, for underdoped samples T_c and T^* of YBCO are clearly separated.

The microstructure[12–14] and the low temperature dependence of the dielectric constant[8] of a PZT/YBCO heterostructure with *optimally doped* YBCO layers with T_c of 91 K had been studied in the past.[14,8] For easy comparison, one example of such a PZT/YBCO sample, which had been prepared in a two-target rf/dc magnetron sputtering system and annealed at oxygen pressure close to 1×10^5 Pa and at $\sim 480\,^\circ$C for 30 min,[14,8] will be given in this paper further below.

The PZT/YBCO and PZ/YBCO heterostructures with *underdoped* YBCO layers were prepared on $SrTiO_3(001)$ substrates in a multitarget pulsed laser deposition (PLD) system.[15] Fully oxygenated YBCO films were deposited on $SrTiO_3(001)$, and immediately afterwards the dielectric PZT or PZ layers were deposited onto the YBCO. The YBCO was deposited at 760 °C under 50 Pa oxygen pressure, then annealed at 450 °C under 8×10^4 Pa oxygen pressure for 30 min. However, the final oxygen stoichiometry in the YBCO layers was determined by the oxygen pressure used during the deposition of the dielectric layer and the subsequent cooling process. We have chosen growth conditions to guarantee optimal epitaxial quality of PZ and PZT. Thin films of PZT are difficult to produce because of the low Pb vapor pressure. Furthermore, as evident from the phase diagram,[16] PZ needs a lower temperature than PZT. Thus, the growth conditions, which we have chosen for PZ and PZT, are slightly different. Two ceramic targets, with nominal composition of $Pb_{1.05}(Zr_{0.53}Ti_{0.47})O_{3.05}$ and $PbZrO_3$, were used for the pulsed laser deposition. The PZ layers were deposited at 300 °C under 10 Pa oxygen pressure followed by a brief annealing at 655 °C in 8×10^4 Pa oxygen pressure, before cooling down to the room temperature by switching off the power of the heater. The PZT layers were deposited at 580 °C under 12 Pa oxygen pressure, then the power of the heater was switched off and the thus prepared heterostructures were cooling down to room temperature without increasing the oxygen pressure and without any further annealing afterwards. Thus prepared PLD samples are referred to as nonfully-oxygenated hereafter, in contrast to the fully-oxygenated PZT/YBCO (PZ/YBCO) samples with $T_c = 91$ K for YBCO layers, which were annealed after the

TABLE I. Lattice constants of perovskite PZT, PZ, YBCO, and $SrTiO_3$.

	PZT (nm)[a]	**PZ** (nm)[a]	**YBCO** (nm)[b]	$SrTiO_3$ (nm)[c]
a	0.408	0.415	0.3817	0.3905
b	0.408	0.415	0.3883	0.3905
c	0.408	0.410	1.1633	0.3905

[a]Reference 16.

[b]R. M. Hazen, in *Physical Properties of High Temperature Superconductors II*, edited by D. M. Ginsberg (World Scientific, Singapore, 1990), pp. 121–198.

[c]J. G. Bednorz and H. J. Scheel, J. Cryst. Growth **41**, 5 (1977).

deposition of dielectric PZT (PZ) layers at ambient pressure of oxygen and at $\sim 450\,^{\circ}C$.

PZT, PZ, YBCO, and $SrTiO_3$ are all perovskite materials with a close match of their lattice constants (cf. Table I) and thermal expansion coefficients, both prerequisites for a good epitaxial quality of the PZT/YBCO and PZ/YBCO heterostructures. Furthermore, PZ and PZT belong to a solid solution, with orthorhombic structure for PZ and rhombohedral structure for PZT. The PZT composition, which we have chosen, is right at the morphotropic phase boundary. Otherwise, PZ and PZT are chemically very similar and thus bond to YBCO with quite similar behavior. Most importantly, PZT is ferroelectric and PZ antiferroelectric. The consequences of this will be discussed further below.

Our PLD films were characterized by x-ray diffraction (XRD) (Siemens D5000), atomic force microscopy (AFM) (Digital Instruments Dimension 3100 with NanoScope III Electronics), scanning electron microscopy (SEM) (Leica Cambridge Stereoscan 420), and high resolution transmission electron microscopy (HRTEM) (Philips CM20-FEG) in both planar and cross-sectional views.[17] The PZT/YBCO and PZ/YBCO heterostructures are epitaxial and single-phase, revealed by the XRD as shown in Fig. 1 for the 120/120 nm thick heterostructures. The oxygen concentration in YBCO layers as derived from *c*-axis lattice constants[18] are $\delta \approx 0.2$ and 0.5 for PZ/YBCO and PZT/YBCO, respectively, which are consistent with that deduced from their T_c values.[19] The PZT and PZ layers are dense with isolated pinholes as observed by SEM and AFM. However, the PZ film is rougher and has more pinholes than the PZT film. The pinhole density in the PZ film is about 4 times that in the PZT film. The HRTEM cross-sectional images of a PZT/YBCO and a PZ/YBCO specimen, both of which are 120/120 nm thick, are given in Fig. 2. Similar microstructural features for both samples can be observed: (1) The interfaces of PZT/YBCO and PZ/YBCO are sharp, without indications of intermixing layers. (2) Parts of the images at the interface of PZT/YBCO or PZ/YBCO suggest that the lattices of PZT and PZ layers are distorted by the interface stress field due to the lattice mismatch of the PZT or PZ layers with the YBCO layers. (3) Similar defects along the film growth direction can be observed for both, PZT and PZ layers. (4) The Fourier filtered TEM images reveal edge dislocations close to the interface with densities of $>10^{12}/cm^2$ for the PZT and PZ films. More details on the deposition procedure and the microstructural characterization of the heterostructures are reported elsewhere.[17]

Au contacts were prepared on the dielectric films *ex situ* by evaporation. We used 200 nm Au pads and 120 nm YBCO layers, but varied the PZT and PZ layer thickness (60, 120, and 180 nm). A schematic drawing of the resulting thin film capacitor structure is shown in Fig. 3.[20] Superconducting transition temperatures were determined by susceptibility measurements with a Magnetic Property Measurement System SQUID magnetometer. With the samples mounted on a helium flow-through cryostat the capacitance *C* of the thin film structure was determined by an HP 4284A LCR meter for frequencies ranging from 1 to 1000 kHz. The experimen-

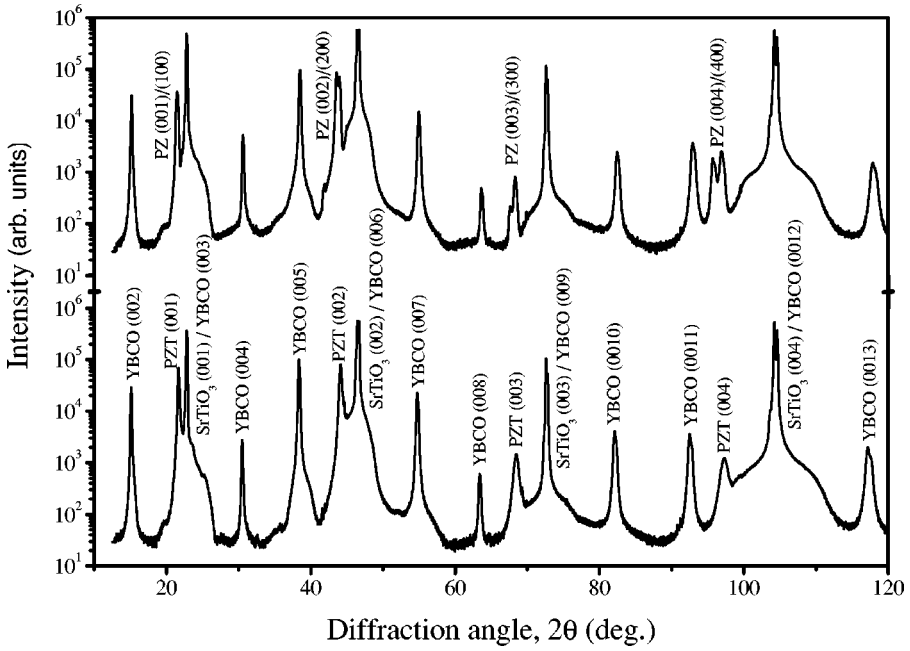

FIG. 1. XRD $\Theta-2\Theta$ scan with the intensity scaled logarithmically for the 120/120 nm thick PZ/YBCO heterostructure (upper graph) and PZT/YBCO heterostructure (lower graph) on $SrTiO_3(001)$ using $Cu\,K_\alpha$ radiation.

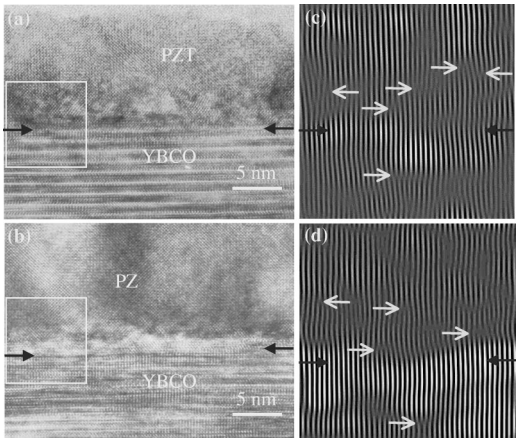

FIG. 2. Cross-sectional HRTEM images of (a) PZT/YBCO and (b) PZ/YBCO heterostructures, revealing sharp interfaces as indicated by the black arrows. (c),(d) Properly Fourier filtered parts of the images marked in (a) and (b), respectively, show dislocation networks with density of $>10^{12}/\mathrm{cm}^2$ close to the interfaces.

tal results presented here have been obtained at 100 kHz for all the samples (see text below). However, despite the fact that the magnitude of the capacitance anomaly shows some frequency dependence, basically the same behavior in terms of temperature dependence, onset temperature, etc. was observed for all other frequencies used for the capacitance measurement. The frequency-dependence will be reported in detail elsewhere. The dielectric constant ε_r can be obtained from the measured capacitance C with the help of the known area of the electrodes A, thickness d of the PZT or PZ layer, and the vacuum dielectric constant ε_0 via

$$\varepsilon_r = \frac{2d \cdot C}{A \cdot \varepsilon_0}. \tag{1}$$

In this paper, we concentrate on the heterostructures with *underdoped* YBCO layers. However, for convenience we reproduce the results obtained for the temperature dependence of the dielectric constant of an fully-oxygenated PZT/YBCO (120/120 nm) sample, i.e., with *optimally doped* YBCO layer ($T_c = 91$ K) as already indicated above.[8] As can be seen in Fig. 4, a strong increase of the dielectric constant is observed for the PZT film at a temperature roughly about 10 K above the superconducting transition. The dielectric constant reaches a maximum at 91 K, which corresponds to $T_{c,0}$, with

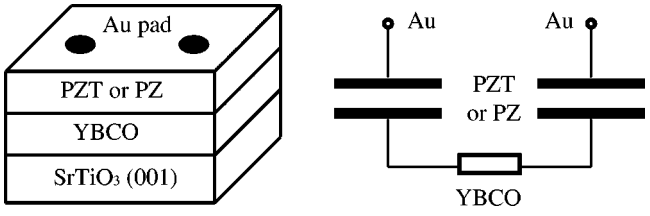

FIG. 3. Two thin film capacitors, with PZT or PZ dielectric layer, are connected in series by the YBCO layer. Au contacts, 1 mm in diameter and 5 mm apart from each other, are deposited on the integrated thin-film structure with a total lateral size on 5 $\times 10$ mm^2 on intrinsic, insulating, 1 mm thick $SrTiO_3$ substrates.

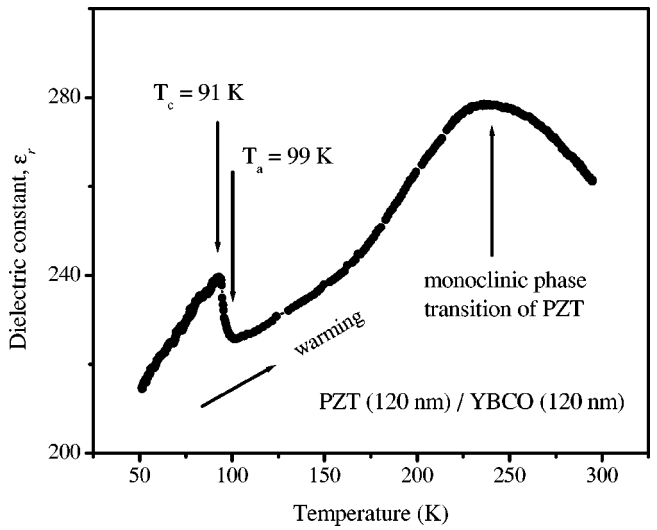

FIG. 4. Temperature dependency of ε_r measured at 100 kHz for an fully-oxygenated PZT/YBCO (120/120 nm) sample with T_c of 91 K.

a total increase of the dielectric constant $\approx 7\%$. The hump in the dielectric constant around 240 K can be assigned to the monoclinic phase transition of the PZT.[21]

The results for three nonfully-oxygenated PZT/YBCO samples with thickness of 60/120 nm, 120/120 nm, and 180/120 nm and one nonfully-oxygenated PZ/YBCO sample (120/120 nm), i.e., with *underdoped* YBCO layers, are shown in Fig. 5. Compared to the fully-oxygenated sample, a stronger increase ($\approx 30\%$) of the capacitance is observed for the 60 nm and 120 nm PZT films, which starts ≈ 10 K above T_c, and reaches the maximum at about T_c [cf. Figs. 5(a) and 5(b)]. For the 180 nm PZT film, the anomaly in the dielectric constant is much weaker [cf. Fig. 5(c)], but closer inspection shows that it exhibits the same dependency on T_c as for the thinner films. Thus, we can summarize at this point already that the temperature at which the observed anomaly happens, depends on T_c. This suggests a superconductivity-related mechanism. However, while the anomaly reaches a maximum at T_c, it starts at temperature T_a, which is about 10 K higher than $T_{c,0}$.

The observed anomaly must originate either from a decrease in d or an increase in ε_r, because ε_0 and A do not change with temperature [cf. Eq. (1)]. A decrease in the "effective" layer thickness d could be caused by the proximity effect: within a certain depth, the interfacial region of the dielectric becomes superconducting leading to a decrease of the *effective* thickness of the dielectric layer. A capacitance change at T_c was found for all the PZT samples with different thickness of the PZT layers. In order for the proximity effect to be responsible for the increase in capacitance for the 120 nm film, more than 30 nm of the PZT film must have become superconducting, which is impossible.[22] However, the proximity effect can be directly ruled out, since, more importantly, its contribution must be very small, as revealed by the PZ samples. No evident anomaly but a very tiny di-

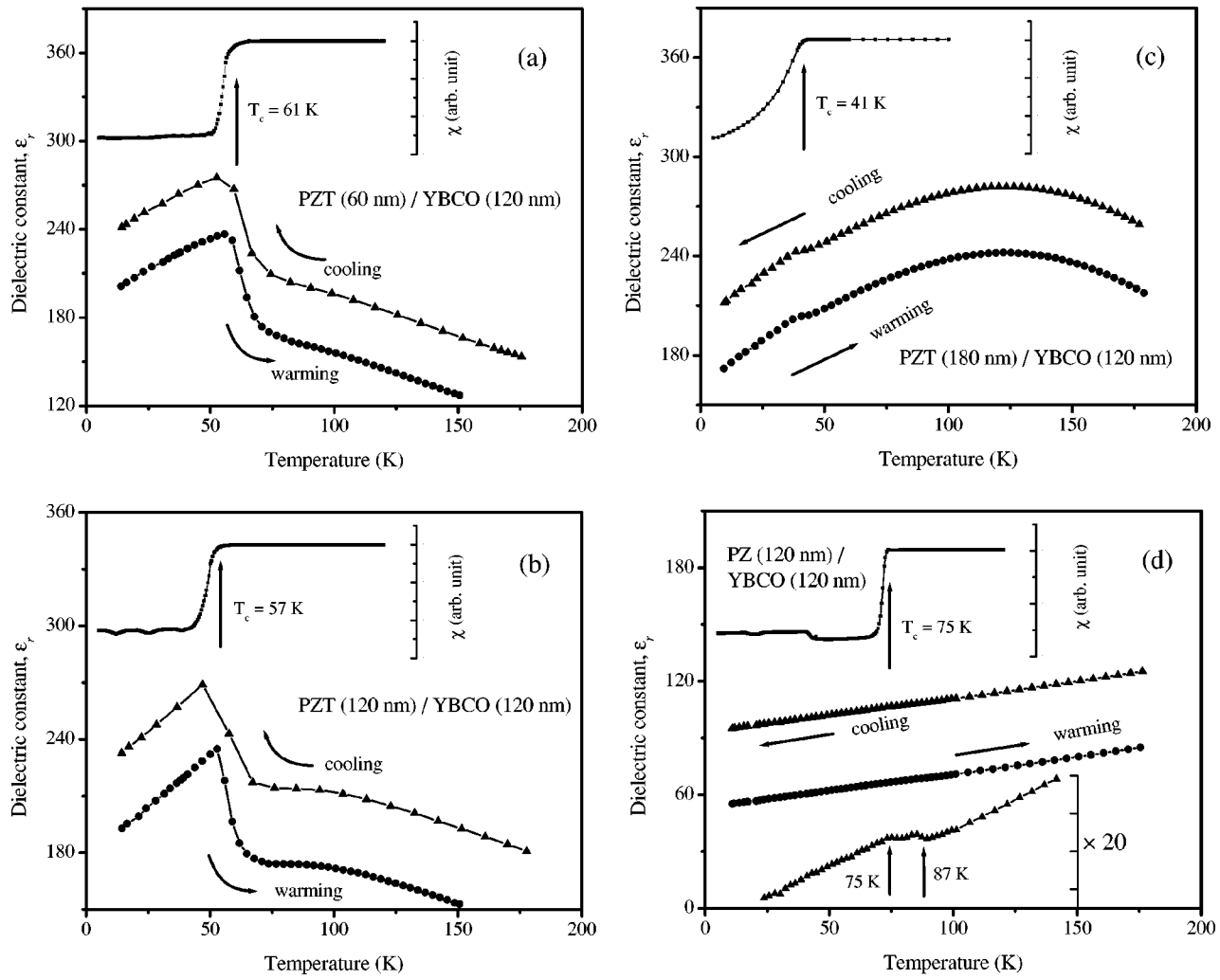

FIG. 5. Temperature dependency of ε_r measured at 100 kHz for nonfully-oxygenated heterostructures with oxygen deficient YBCO layers: (a) PZT/YBCO, 60/120 nm,$T_c=61$ K; (b) PZT/YBCO, 120/120 nm,$T_c=57$ K; (c) PZT/YBCO, 180/120 nm,$T_c=41$ K; (d) PZ/YBCO, 120/120 nm,$T_c=75$ K. There is no observable hysteresis for the cooling, warming cycle and the lower curve is vertically displaced downward by $\varepsilon=40$ for clarity. The results of the susceptibility measurements are shown as insets. The lower inset in (d) shows the small change of ε_r around 75 K by subtraction of the linear $\epsilon(T)$ dependence and a vertical expansion by a factor of 20.

electric kink close to T_c can be identified for all the three PZ samples [cf. Fig. 5(d), and see text below]. Weak ferroelectricity in the PZ film[23] may contribute to this tiny dielectric kink, too. Nevertheless, any possible contribution of the proximity effect must be very small. STO undergoes an antiferrodistortive phase transition at low temperature and one might suspect that this maybe related to the observed anomaly. However, the phase transition of STO occurs at 105 K (Ref. 24) and is a prototype of a second-order phase transition, with a slow and continuous change of the STO lattice constants with decreasing temperature.[25] Thus, there is no sudden variation. Furthermore, whereas the STO phase transition occurs at around 105 K, the anomaly which we observe scales with the T_c of the YBCO films within a range of 41–91 K. This leaves as the only explanation a change of ε_r in the dielectric film at the superconducting transition.

In order to understand the different behavior for PZT and PZ we have to recall their properties. The phase diagram of $Pb(Zr_{1-x}Ti_x)O_3$ shows (below about 500 K) a variety of phases:[16] The material is orthorhombic and antiferroelectric for $x=0$ (PZ); with x increasing, it becomes rhombohedral ferroelectric close to 0.1 and exhibits a so-called morphotropic phase boundary between the ferroelectric rhombohedral and ferroelectric tetrahedral phase at around $x=0.5$. The ferroelectric phases are, of course, also piezoelectric[26] and an external stress will change the electric polarization and thus the dielectric constant and the measured capacitance. Important for our present approach, *this is not the case* for the AFE (Ref. 27) phase of PZ which is centrosymmetric and thus not piezoelectric. In our opinion, the only explanation left for explaining the jump in the dielectric constant for the FE material at the superconducting transition is a change of stress, the magnitude of which we will estimate in the following.

The Gibbs free energy per unit volume of piezoelectrics can be expressed as,[16,26]

$$G = G_0 + \sum_i \left(\frac{1}{2} E_i \cdot P_i\right) + \sum_i \left(\frac{1}{2} F_i \cdot S_i\right)$$

$$= G_0 + \sum_i \frac{P_i^2}{2\chi_0} + \sum_{i,j} \frac{F_i^2}{2c_{ij}}, \quad (2)$$

with the ground state free energy G_0, electric field E_i, polarization P_i, stress tensor F_i, strain tensor S_i, and elastic constants c_{ij}. Under a weak electric field, the inverse dielectric susceptibility χ^{-1} equals $(\partial^2 G/\partial P_i^2)|_{P=0}$, then,

$$\frac{\partial G}{\partial P_i} = \frac{P_i}{\chi_0} + \sum_{i,j} \frac{1}{c_{ij}} \cdot \frac{\partial F_i}{\partial P_i} \cdot F_i, \quad (3)$$

and thus,

$$\frac{1}{\chi} = \frac{1}{\chi_0} + \sum_{i,j} \frac{1}{c_{ij}} \left[\frac{\partial^2 F_i}{\partial P_i^2} \cdot F_i + \left(\frac{\partial F_i}{\partial P_i}\right)^2 \right], \quad (4)$$

in which $\partial F_i/\partial P_i$ and $\partial^2 F_i/\partial P_i^2$ are the piezoelectric strain constants g_{ij} and the electrostrictive coefficients Q_{ij}, respectively.

It is obvious that the $\partial F_i/\partial P_i$ term in Eq. (3) equals zero for the AFE, and therefore an external stress field does not introduce any significant change of the dielectric constant. However, for piezoelectric materials such as ferroelectrics, an external stress induces a stress-proportional change of the dielectric constant. For PZT, a compressive stress in the a/b-plane will decrease ε_r.[16] It is important to realize at this point, that the epitaxial PZT and PZ films on YBCO are *compressively stressed* given their larger lattice constants. The *enhancement* of ε_r which we observed means that the lateral compressive stress component F_1 *is released* in the FE film,[16] whereby the polarization of the FE is influenced in such a way that the dielectric constant $\varepsilon_r = 1 + \chi = \varepsilon_{33}^S/\varepsilon_0$ increases in the *c*-direction.

We notice that, for nonfully-oxygenated PZT/YBCO PLD samples, the dielectric hump at around 240 K disappears. This suggests that without oxygen annealing after the deposition of PZT not only the YBCO layers are oxygen deficient, but that a higher density of defects may be present in the PZT layers. This assumption is supported by the high density of dislocations observed by HRTEM.[17] Furthermore, it is known that vacancies in the PZT ceramics increase the mobility of domain-wall and thus decrease the threshold for stress release.[28] Therefore, it may not be surprising that the amount of stress released in the nonfully-oxygenated PZT/YBCO samples at close to T_c is larger in comparison with the fully-oxygenated sample [cf. Figs. 4 and 5(b)].

From Eq. (4), we can estimate the magnitude of stress release in the PZT. With a change in $1/\chi$, i.e., $(1/\chi)_{|T>T_a} - (1/\chi)_{|T<T_c} = 0.001$, $c_{33} = 134$ GPa,[16] and $Q_{33} = 2.0$ $m^4 \cdot C^{-2}$,[29] we calculate a release of stress of ≈ 70 MPa in the nonfully-oxygenated PZT layers [60 and 120 nm thick, cf. Figs. 5(a) and 5(b)]. Obviously, the PZT film represents a very sensitive probe for stress changes in the YBCO film. Employing the elastic constants of YBCO at room temperature,[30] we estimate a strain change of 3×10^{-4} in the YBCO layer associated with this stress release. The same calculation reveals a release of stress of ≈ 20 MPa in the fully-oxygenated 120 nm PZT layer (cf. Fig. 4).

The 180 nm thick PZT film exhibits at room temperature the highest ε_r value among all the three samples of different PZT layer thickness. This is an indication that the thicker PZT film is much less (in our case compressively) stressed at room temperature. This is, in fact, expected for any epitaxial systems. The strain energy, which accumulates with thickness, is reduced by the formation of dislocations. Thus, the thicker the epitaxial films become, the less they are constrained by the substrate. For epitaxial $Ba_xSr_{1-x}TiO_3$ (BST) thin films[31,32] it was recently found that the dielectric constant of the BST film depends on its *c*-axis lattice constant and defects inside the films. In accordance with our reasoning above, it was suggested that the release of the internal stress in the thicker BST films is the reason for the increase of the dielectric constant with layer thickness. Thus, for our 180 nm PZT film, we observe a smaller release of the stress close to the T_c [cf. Fig. 5(c)], since the amount of internal stress is already drastically reduced in comparison with the thinner films.

The underlying mechanism for the stress change is not conclusively established, however, our present investigations shed some light on it. The fact that the anomaly starts at a temperature close to T_c with a maximum at T_c for both the optimal doped and the underdoped YBCO clearly relates the effect to the superconducting transition. A simple change in the elastic constants cannot be the reason since a *stiffening* of the shear modulus is observed below T_c.[33] The other possibility, a lattice constant change in the YBCO at T_c caused by a structural transition as, e.g., reported by Meingast *et al.*,[34] is not likely, either, since the induced strain change can be estimated to be $<1 \times 10^{-5}$,[34] much smaller than what we observe. Another explanation is a ''plasticity enhancement'' in the superconducting state, i.e., the movement of dislocations, which requires also a redistribution of electric charge, can occur more easily in the superconducting state, thus leading to a softening of the material. We believe that this mechanism may best explain our experimental observations: (1) For all the samples studied, which have an identical thickness of the YBCO layers, an equal release of the residual stress inside the YBCO layers at around T_c is expected. (2) Because PZ is in principle not piezoelectric and thus not sensitive to a stress change, no evident change in the dielectric constant can be observed [cf. Fig. 5(d)]. (3) For the PZT layers, the stress release, as determined from the change in dielectric constant, is of different magnitude for the 60 nm PZT, the fully-oxygenated and the nonfully-oxygenated 120 nm PZT, and the 180 nm PZT, because of the differences in the domain-wall mobility [cf. Figs. 4 and 5(b)] and the much lower internal stress in the thicker films [cf. Fig. 5(b) and 5(c)]. A change of threshold for inelastic deformation has actually been reported to happen for YBCO ceramics around

the superconducting transition temperature.[4] Finally, the reason for our finding that this anomaly commences already at a temperature several degrees above T_c is not clear at the moment. However, note in this context that the electron–phonon coupling, reported recently for HTS cuperates, was found to persist at temperatures significantly higher than T_c.[35]

In conclusion, by employing piezoelectric PZT as a probe, we observed a pronounced change of capacity in our integrated capacitor microstructures at the superconducting transition temperatures of the YBCO, which we associate with a change of stress in YBCO close to T_c. We corroborated this assignment by comparing the dielectric response of PZT and PZ thin film capacitors at the superconducting transition of YBCO electrode layers with different transition temperatures. The dielectric constants of Au/PZT/YBCO integrated thin film capacitors were found to increase, up to $\approx 30\%$, starting at a temperature ≈ 10 K above the T_c of YBCO, while basically no changes can be observed for Au/PZ/YBCO. A very small kink for the antiferroelectric, nonpiezoelectric PZ can be assigned to the proximity effect or interfacial ferroelectricity of the PZ layer. By varying the transition temperatures of YBCO in the range of 41–91 K, we showed that the capacitance anomaly clearly scales with T_c, starting about 10 K above T_c in all cases. The PZT layer represents a very sensitive stress sensor and the anomaly is consistent with a stress change of up to 70 MPa, which corresponds to a strain change of 3×10^{-4} in the YBCO layer.

This work was supported by the German BMBF under Contract No. SE8GUA5. Skillful technical assistance by Gisela Siegle, Eva Brücher, Wolfgang Stiepany, and the technology group of H.-U. Habermeier at the MPI-FKF was instrumental in this study.

*Author to whom correspondence should be addressed. Electronic address: zegenhagen@esrf.fr

[1] L. D. Landau and E. M. Lifshitz, *Statistical Physics* (Pergamon, Oxford, 1980).

[2] H. Kojima and T. Suzuki, Phys. Rev. Lett. **21**, 896 (1968).

[3] For review, see, e.g., F. R. N. Nabarro and A. T. Quintanilha, in *Dislocations in Solids V*, edited by F. R. N. Nabarro (North-Holland, Amsterdam, 1980), pp. 193–242; V. I. Startsev, in *Dislocations in Solids VI*, edited by F. R. N. Nabarro (North-Holland, Amsterdam, 1983), pp. 143–233.

[4] N.N. Peschanskaya, B.I. Smirnov, V.V. Shpeizman, and P.N. Yakushev, Sov. Phys. Solid State **30**, 2014 (1988); N.N. Peschanskaya, B.I. Smirnov, and P.N. Yakushev, *ibid.* **31**, 1446 (1989).

[5] G.A. Alers, O. Bunk, and B.R. Tittmann, Phys. Rev. Lett. **23**, 290 (1969).

[6] T.S. Hutchison and A.T. Pawlowicz, Phys. Rev. Lett. **25**, 1272 (1970).

[7] N.J. Wu, H. Lin, K. Xie, X.Y. Li, and A. Ignatiev, Physica C **232**, 151 (1994).

[8] B.R. Zhao, L.X. Cao, J.H. Jiang, Y. Xu, K. Ma, L. Li, Y. Zhu, D.F. Zhang, J.H. Zhao, X.J. Li, B. Xu, Y.Z. Zhang, T. Yang, and Z.X. Zhao, Physica C **282-287**, 713 (1997).

[9] H. Oyanagi and J. Zegenhagen, J. Supercond. **10**, 415 (1997).

[10] T. Ito, K. Takenaka, and S. Uchida, Phys. Rev. Lett. **70**, 3995 (1993).

[11] See, e.g., H. Oyanagi, J. Zegenhagen, and T. Haage, in *Stripes and Related Phenomena*, edited by A. Bianconi and N. Saini (Kluwer Academic, Dordrecht, 2000), p. 227.

[12] R. Ramesh, A. Inam, W.K. Chan, F. Tillerot, B. Wilkens, C.C. Chang, T. Sands, J.M. Tarascon, and V.G. Kermidas, Appl. Phys. Lett. **59**, 3542 (1991).

[13] For a recent review, L. Li, Mater. Sci. Eng., R. **29**, 153 (2000).

[14] L.X. Cao, Y. Xu, B.R. Zhao, L.P. Guo, J.Z. Liu, B. Xu, F. Wu, L. Li, Z.X. Zhao, A.J. Zhu, Z.H. Mai, J.H. Zhao, Y.F. Fu, and X.J. Li, Supercond. Sci. Technol. **9**, 310 (1996).

[15] Q.D. Jiang and J. Zegenhagen, Surf. Sci. **338**, L882 (1995).

[16] *Landolt-Börnstein New Series III/16a*, edited by K.-H. Hellwege and A. M. Hellwege (Springer-Verlag, Berlin, 1981).

[17] L.X. Cao, Y.L. Qin, A. Deac, I. Snigireva, and J. Zegenhagen, J. Phys.: Condens. Matter **14**, 3093 (2002).

[18] J.D. Jorgensen, B.W. Veal, A.P. Paulikas, L.J. Nowicki, G.W. Crabtree, H. Claus, and W.K. Kwok, Phys. Rev. B **41**, 1863 (1990).

[19] J. Tallon and N. Flower, Physica C **204**, 237 (1993).

[20] For the Au/PZT/YBCO thin film capacitor, carrier density and work function of the Au and YBCO electrodes are different, which results in two different barriers at interfaces of Au/PZT and YBCO/PZT. However, the series array of two such thin film capacitors leads to a symmetrical structure, Au/PZT/YBCO/PZT/Au, in which the different charging process at the barriers compensate each other during the AC measurement.

[21] B. Noheda, D.E. Cox, G. Shirane, J.A. Gonzalo, L.E. Cross, and S.-E. Park, Appl. Phys. Lett. **74**, 2059 (1999); B. Noheda, J.A. Gonzalo, L.E. Cross, R. Guo, S.-E. Park, D.E. Cox, and G. Shirane, Phys. Rev. B **61**, 8687 (2000).

[22] The thickness of the dielectric film which may become superconducting due to the proximity effect is determined by the coherent lengths of YBCO, which is <1 nm.

[23] I. Kanno, S. Hayashi, M. Kitagawa, R. Takayama, and T. Hirao, Appl. Phys. Lett. **66**, 145 (1995); P. Ayyub, S. Chattopadhyay, R. Pinto, and M.S. Multani, Phys. Rev. B **57**, R5559 (1998).

[24] H. Unoki and T. Sakudo, J. Phys. Soc. Jpn. **23**, 546 (1967); G. Shirane and Y. Yamada, Phys. Rev. **177**, 858 (1969).

[25] L.X. Cao, E. Sozontov, and J. Zegenhagen, Phys. Status Solidi A **181**, 387 (2000).

[26] B. Jaffe, W. R. Cook, and H. Jaffe, *Piezoelectric Ceramics* (Academic, London, 1971).

[27] C. Kittel, Phys. Rev. **82**, 729 (1951).

[28] R. Gerson, J. Appl. Phys. **31**, 188 (1960).

[29] V. Sundar, N. Kim, C. A. Randall, R. Yimnirun, and R. E. Newnham, in Proceedings of IEEE-International Symposium on the Applications of Ferroelectrics (ISAF-1996), Rutgers University, 1996, p. 935.

[30] M. Lei, J.L. Sarrao, W.M. Visscher, T.M. Bell, J.D. Thompson, A. Migliori, U.W. Welp, and B.W. Veal, Phys. Rev. B **47**, 6154 (1993).

[31] C.L. Canedy, H. Li, S.P. Alpay, L. Salamanca-Riba, A.L. Roytburd, and R. Ramesh, Appl. Phys. Lett. **77**, 1695 (2000).

[32] H. Li, A.L. Roytburd, S.P. Alpay, T.D. Tran, L. Salamanca-Riba, and R. Ramesh, Appl. Phys. Lett. **78**, 2354 (2001).
[33] H.M. Ledbetter, M.W. Austin, S.A. Kim, T. Datta, and C.E. Violet, J. Mater. Res. **2**, 790 (1987).
[34] C. Meingast, O. Krauf, T. Wolf, H. Wühl, A. Erb, and G. Müller-Vogt, Phys. Rev. Lett. **67**, 1634 (1991).
[35] A. Lanzara, P.V. Bogdanov, X.J. Zhou, S.A. Keller, D.L. Feng, E.D. Lu, T. Yoshida, H. Eisaki, A. Fujimori, K. Kishio, J.-I. Shimoyama, T. Noda, S. Uchida, Z. Hussain, and Z.-X. Shen, Nature (London) **412**, 510 (2001).